GRAPHENE-LIKE FILMS FROM CARBON BLACK: A FACILE AND CONVENIENT ROUTE

M. Alfè*, V. Gargiulo*, R. Di Capua**, A. Ciajolo*

alfe@irc.cnr.it

* Istituto di Ricerche sulla Combustione (IRC)-CNR, Napoli, Italy
** SPIN-CNR UOS Napoli, via Cintia, I-80126, Napoli, Italy; Dipartimento S.pe.S.,
Università del Molise, Campobasso, Italy

Graphene attractive chemical-physical properties are largely exploited to fabricate electronic and optoelectronic devices such as window electrodes for the production of solid-state dye sensitized solar cells, light emitting diode (LED) and liquid crystals. Graphene is also involved in the fabrication of energy-storage materials and mechanical resonators. Graphene can also be used as channel material for the next generation of field emission transistors (FET) or as conductive sheet upon which nanometer scale devices may be patterned to create single electron or few electron transistors [1-3].

The bottleneck in the graphene-based technology is its production on a large scale. Various approaches have been used to produce graphene including one-step graphite exfoliation, chemical vapor deposition (CVD) of methane gas, graphite stamping, graphite oxide reduction and carbon nanotube unzipping. Among these, the production of graphite oxide (GO) from graphite powder and its further reduction (through chemical, thermal, or ultraviolet-assisted reduction methods) to graphene-like material is a convenient and economic way of graphene-like sheet fabrication [1-3].

Aim of this study is to propose a convenient synthesis of graphene-like films starting from water suspension of oxidized carbon black (CB). The selected oxidative treatment provides the partial demolition of the CB microstructure and the functionalization at the edge of the basal planes of the graphitic layers [4] and not on them. In this way, differently from GO, the oxidized CB preserves the original graphitic network useful for the conductivity and electronic properties. The method offers scalability and potential high-volume production of graphene-like films at reduced costs.

Experimental

Starting material. The selected CB (Phillips Petroleum Co., furnace carbon black, named N110 according to ASTM classification) is arranged in chain-like aggregates of spherical primary particles (15-20 nm) with a narrow size distribution, as shown by transmission electron microscopy (TEM) [5]. The nanoscale organization of carbon black primary particles is typical of a disordered carbon. More organized regions are observed with a concentric organization of the stacked graphitic layers extending throughout each primary particle.

Methods. H/C atomic ratio of CB and HNP materials were measured by a Perkin–Elmer 2400 CHNSO elemental analyzer. The thermal stability of the samples was characterized by thermogravimetric analysis (TGA); all measurements were performed on a Perkin–Elmer Pyris 1 Thermogravimetric Analyzer. The carbonaceous materials were heated in oxidative environment (air, 30 mL min-1) from 30 °C up to 750 °C at a rate of 10 °C min^{-1} with and without a preheating in nitrogen atmosphere (N_2, 40 mL min^{-1} from 30 °C up to 750 °C, 10 °C min^{-1}). Fourier Transform Infrared (FTIR) spectra were recorded on a Nicolet iS10 spectrometer using the attenuated total reflectance (ATR) method. The measurements were performed on the powdered samples without KBr addition in the 600-4000 cm^{-1} range by using a germanium crystal. Electron transmission microscopy (TEM) images were acquired on a JEOL 2011 operating at 200 kV using LaB_6 filament. Samples for AFM imaging were prepared by drop-casting dilute HNP90R water dispersions (2 mg mL^{-1}) onto freshly cleaved mica substrates. AFM images were acquired on n XE100 Park instrument operating in non-contact mode (amplitude modulation, silicon nitride cantilever from Nanosensor).

Sample preparation and purification. CB was oxidized according to the procedure reported by Kamegawa [6]. The CB powder was treated with hot nitric acid (67 wt.%, 100 °C) under stirring for 90 hours. The product had a dark brown appearance and it was not as opaque black as the pristine CB. The hydrophilic product at the end of the isolation procedure was dried and labeled as HNP90.

The reduction of HNP90 was performed by adapting the procedure proposed for GO by Stankovich [7]. The HNP90 water dispersion was heated in an oil bath at 100 °C under reflux for 24 h with hydrazine hydrate. The product was isolated, dried and labeled as HNP90R. More detailed information about the sample preparation were reported in Alfè et al. [8]. The dried HNP90R was insoluble in water and in the most common organic solvents, both polar and apolar (water, ethanol, NMP, dichloromethane, heptane, DMF). This was attributed to an increase of hydrophobicity of the material caused by a decrease in the polar functionalities on the surface and consequent intimate self-assembling interaction between the restored graphitic planes.

Results

Table 1 reports the elemental composition of CB and HNP. The hydrogen content tends to increase from 0.48 to 1.21 suggesting the reduction of the dimension of the graphitic basal planes. The increase of the H/C ratio from 0.058 (raw CB) to 0.27 (HNP90) confirms this hypothesis. The oxidation results in the introduction of oxygenated functional groups (hydroxyl, carboxylic, carbonylic) as testified by the increase of the oxygen content from 0.6% (raw CB) to 44% (HNP90). The increase of nitrogen from 0.04% (raw CB) to 1.12% (HNP90) as a consequence of the introduction of nitro groups is also observed.

Table 1. Composition of raw CB and HNP.

	C (wt. %)	H (wt. %)	O (wt. %)	N (wt. %)	O/C
CB	98.9	0.48	0.59	0.04	0.0045
HNP90	53.6	1.21	44.1	1.12	0.62
HNP90R	52.9	1.40	39.7	6.09	0.56

The chemical reduction of HNP90 with hydrazine also introduce nitrogen functionalities likely in the form of hydrazones or similar structures, leading to an increase of nitrogen percentage from 1.12 (HNP90) to 6.09 (HNP90R). Is it noteworthy that the oxygenated functionalities are not completely removed upon the chemical reduction. However it represents an expected result, since it is well known that CB oxidized with nitric acid has not oxygen atoms on basal planes in the form of epoxides, but only on their edges [4]. The H/C ratio kept nearly constant (0.27-0.32) suggesting that the size of the graphitic units remains rather unchanged.

ATR-FTIR spectra of HNP90, HNP90R and raw CB are reported in Figure 1. The spectra are baseline corrected and shifted for clarity. The spectra are broad in shape as a consequence of the presence of a complex carbon network. The most characteristic feature of HNP is the presence of the bands attributed to different types of oxygenated functionalities that are completely absent in the raw CB spectrum. The HNP90 spectrum exhibits a broad band in the 3000-3700 cm^{-1} range (O-H stretching vibrations due to carboxylic, phenolic groups and possible adsorbed H_2O). The HNP90R presents a band shift toward lower wavenumbers as a consequence of the N-H stretching band due to the introduction of NH_2 functionalities (hydrazones). Both HNP90 and HNP90R exhibit bands at 1650-1750cm^{-1} (C=O stretching vibrations from carbonyl and carboxylic groups), 1500-1600 cm^{-1} (skeletal vibration of the sp^2 graphitic domains). The intensity of the C=O stretching band is significantly lower in the HNP90R as a consequence of the removal of carboxylic-carbonylic functionalities upon the reductive treatment. The HNP90 spectrum presents an enhanced broad band in the 1300-1100 cm^{-1} regions ascribable to the overlapping of C-OH and C-O stretching vibrations. The reductive treatment also reduces the intensity of the C-O broad band. The presence of nitrogen atoms in the form of nitro groups was certified with the typical bands at 1560 and 1350 cm^{-1} originated by the –NO_2 stretching vibrations [9].

TGA provides information about the thermal stability of the materials, which can be also related to their chemistry. The preheating in nitrogen atmosphere was performed with the aim to decompose the functional groups; the subsequent TG in air allows obtaining information on the temperature oxidation of the graphitic core.
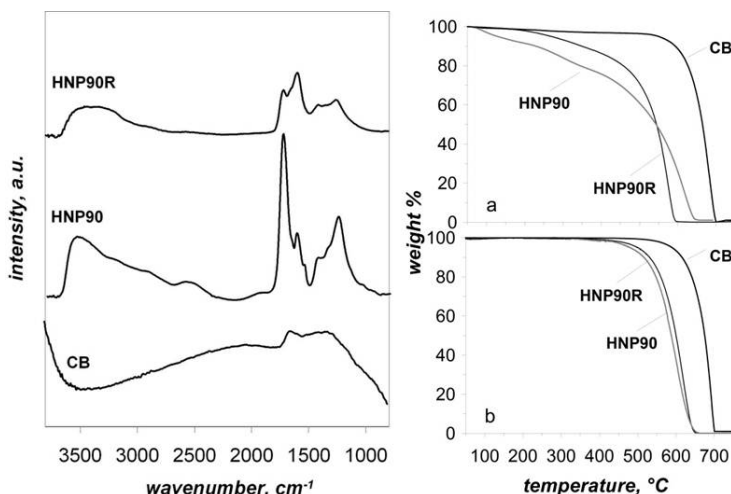
Figure 1. ATR-IR spectra (left) and TGA performed in air without any preheating (right, a) and after a pre-heating in nitrogen atmosphere (right, b) of raw CB, HNP90 and HNP90R.

TGA plots of HNP90 and HNP90R in oxidative environment (air, Figure 1a) show two low temperature weight losses occurring at about 100 °C (10% weight loss) and between 150 and 500 °C (20-40% weight loss). The first one corresponds to the removal of physically adsorbed water while the second represents the decomposition of more stable oxygen functionalities. The mass loss at 150-500 °C is lower in the HNP90R sample as a consequence of the lower number of oxygenated functionalities, partially removed upon chemical reduction. The high temperature mass loss corresponding to the bulk oxidation of HNP occurs at lower temperature with respect to the pristine CB (690 °C) confirming the degradation of the graphitic backbone upon the wet oxidative treatment. The TGA analysis performed in air after heating in N_2 at 750 °C (Figure 1b) indicate that the sample oxidation occurs also in this case at lower temperature with respect to raw CB confirming the degradation of the pristine CB structure. It is noteworthy that the bulk oxidations of HNP90 and HNP90R are comparable suggesting a similar size of the graphitic core.

TEM images of HNP90 (Figure 2b and 2e) show that the carbonaceous backbone of the raw CB (Figure 2a and 2d) is destroyed upon the oxidative treatment and the pristine CB nanostructure arrangement is lost. The HNP90R sample (Figure 2c) consists in large flat areas that are a few layers thick, as the result of HNP90R self-assembling processes after drying.

Lattice fringe analysis of HRTEM images, UV-Vis and Raman spectroscopy, here not shown for lack of room and available elsewhere [8], confirm a decrease in size of the HNP90 and HNP90R π conjugation domains with respect to the pristine CB. The analyses also indicate the preservation of the graphitic network in HNP90 and

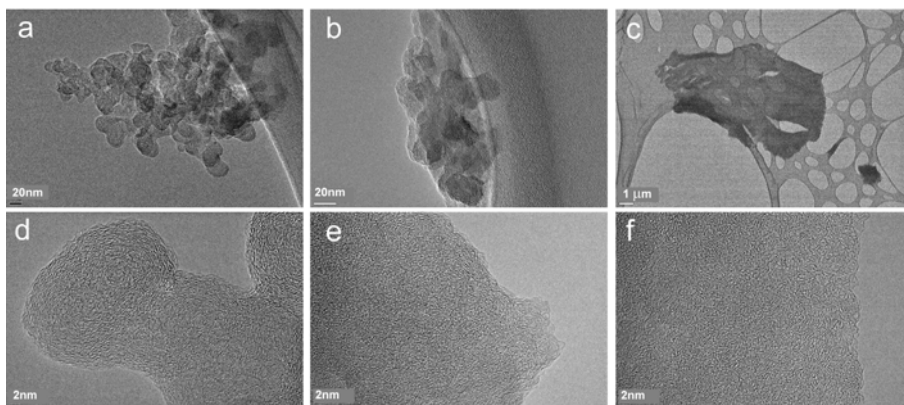reduced HNP90, ascribable to a negligible functionalization at the basal plane of the HNP90 material.

Figure 2. HRTEM images of raw CB (a, d), HNP90 (b, e) and HNP90R (c, f).

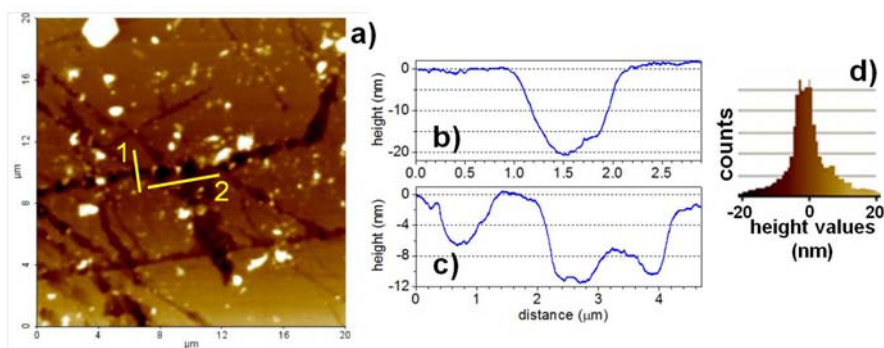AFM measurements (Figure 3) provided information about the surface features of the HNP90R sample.

Figure 3. a) Non-contact AFM topographic image on the HNP90R, 20 μm x 20 μm; b) and c) height profiles, along lines 1 and 2 in the image, respectively; d) histogram of the height values over the whole image.

The self-assembled HNP90R sample is made by pliant sheets that easily conform to any feature of that surface. The diluted sample naturally shrinks during the evaporation of the solvent. Thus, some fractures appear on the surface, likely down the mica substrate, as a result of the film drying process; their depth gives estimation of the thickness of such dropped sample. The roughness on a compact region, estimated by the scan profile reported in Figure 3b, is about 0.5 nm peak to peak over a distance of 1 μm, and of the order of 0.1 nm if considering a root mean square roughness. These values clearly indicate flatness at atomic level. Typically,

the thickness of a graphene-like monolayer obtained by chemical reduction of GO is in the range of 0.6-0.8 nm [10], so the shown film most likely consists of about 25 layers. The light circular-like particles appears on the surface were attributable to the presence of some moisture and impurities coming from the solution or from the environment. The distribution of the measured relative heights gives the histogram reported in Figure 3e. In this plot, the central part is representative of the flat terraces, and its spread must be ascribed to the different number of sheets.

Basic electrical characterization shows the effect of the reduction on the transport properties. Current vs. voltage (I-V) measurements have been carried out in a four contact geometry. Pristine CB and HPN90 did not reveal any electrical current within the sensitivity of our experimental apparatus (Keithley picoammeter Model 6485) up to an applied voltage of 10 V. On the contrary, on the sample HPN90R we observed an ohmic behavior of the I-V characteristic. The resistivity was evaluated by following the Van der Pauw method [11] obtaining a value of 6 $\Omega \cdot$m. This value, however, likely represents an overestimation of the intrinsic resistivity of the material of the film, since the fragmentation of the sample on the micrometer scale leads to a decrease of the effective circulating current for a given voltage in a given geometry.

References
[1] Allen, M.J.; Tung, V.C.; Kaner, R.B. *Chem. Rev.* 110:132-145 (2010)**.**
[2] Huang, X., Yin, Z., Wu S., Qi, X., He, Q., Zhang, Q., Yan, Q., Boey, F., Zhang, H. *Small* 7:1876–1902 (2011).
[3] Zhu, Y., Murali, S., Cai, W., Li, X., Suk J.W., Potts J.R., Ruoff, R.S. *Adv. Mater.* 22:3906–3924 (2010).
[4] Kamegawa, K., Nisiukubo, K., Kodama, M., Adachi, Y., Yoshida, H. *Carbon* 40:1447-1455 (2002**)**.
[5] Santini, E., Ravera, F., Ferrari, M., Alfè, M., Ciajolo, A., Liggieri, L. *Colloids and Surfaces A: Physicochem Eng. Aspects* 365:189-198 (2010**)**.
[6] Kamegawa, K., Nisiukubo, K., Yoshida, H. *Carbon* 36:433-441 (1998**)**.
[7] Stankovich, S., Dikin, D.A., Piner, R.D.; Kohlhaas, K.A., Kleinhammens, A., Jia, Y., Wu, Y., Nguyen, S.T., Ruoff, R.S. *Carbon* 45:1558-1565 (2007**)**.
[8] Alfè, M., Gargiulo, V., Di Capua, R., Chiarella, F., Rouzaud, J.N.,Vergara, A., Ciajolo, A. *ACS Appl. Mater. Interfaces* doi:10.1021/am301197q (2012).
[9] Zawadzki, J. *Carbon* 18:281-285 (1980).
[10] Paredes, J.I., Villar-Rodil, S., Solıs-Fernandez, P., Martınez-Alonso, A., Tascon J.M.D. *Langmuir* 25:5957-5968 (2009).
[11] Van der Pauw, L.J. *Philips Res. Repts.* 13:1-9 (1958).